

# SYSTEM IDENTIFICATION OF SOIL BEHAVIOR FROM VERTICAL SEISMIC ARRAYS

Steven D. Glaser<sup>1</sup>, Sheng-Huoo Ni<sup>2</sup> and Chi-Chih Ko<sup>3</sup>

## ABSTRACT

A down hole vertical seismic array is a sequence of instruments installed at various depths in the ground to record the ground motion at multiple depths during an earthquake. Numerous studies demonstrate the unique utility of vertical seismic arrays for studying in situ site response and soil behavior. Examples are given of analyses made at two sites to show the value of data from vertical seismic arrays. The sites examined are the Lotung, Taiwan SMART1 array and a new site installed at Jingliao, Taiwan. Details of the installation of the Jingliao array are given.

ARX models are theoretically the correct process models for vertical wave propagation in the layered earth, and are used to linearly map deeper sensor input signals to shallower sensor output signals. An example of Event 16 at the Lotung array is given. This same data, when examined in detail with a Bayesian inference model, can also be explained by nonlinear filters yielding commonly accepted soil degradation curves.

Results from applying an ARMAX model to data from the Jingliao vertical seismic array are presented. Estimates of inter-transducer soil increment resonant frequency, shear modulus, and damping ratio are presented. The shear modulus varied from 50 to 150 MPa, and damping ratio between 8% and 15%.

---

<sup>1</sup> Professor, Dept. Civil and Environmental Eng., University of California, Berkeley CA, 94720; [glaser@ce.berkeley.edu](mailto:glaser@ce.berkeley.edu)

<sup>2</sup> Professor, Department of Civil Engineering, National Cheng-Kung University, Tainan, Taiwan, [tonyni@mail.ncku.edu.tw](mailto:tonyni@mail.ncku.edu.tw).

<sup>3</sup> Graduate student, Department of Civil Engineering, National Cheng-Kung University, Tainan, Taiwan.

A new, affordable, hardware monitoring system - TerraScope - is an affordable 4-D down-hole seismic monitoring system based on independent, microprocessor-controlled sensor Pods. The Pods are nominally 50 mm in diameter, and about 120 mm long. An internal 16-bit micro-controller oversees all aspects of instrumentation, eight programmable gain amplifiers, and local signal storage.

Keywords: system identification, vertical arrays, embedded systems, time series, MEMS sensors

## **INTRODUCTION**

Seismic Hazards induced by soil liquefaction during earthquakes are common, with many incidents occurring during the Chi-Chi earthquakes in 1999. Liquefaction resulted in damage to a number of structures and transportation facilities. These events resulted in many studies of soil liquefaction behavior and potential in Taiwan. Since most of these studies took place in the laboratory, the soil behavior observed has to be verified with in-situ test results and observed site behavior. Although there were many liquefaction cases during the Chi-Chi earthquake, no records of vibration and pore water pressure history data was recorded due to the lack of vertical seismic arrays. Since the only vertical seismic array data set is the Wildlife site recording of the 1987 Superstition Hills event (e.g. Brady et al., 1989), the in-situ seismic response and liquefaction criteria during earthquakes are still not well known. Most of investigations were post-liquefaction analysis, and the process from in-situ equilibrium to liquefaction is still an important area of study. The installation of in-situ soil liquefaction monitoring systems is needed.

A down hole vertical seismic array is a sequence of instruments installed at various depths in the ground to record ground motion (generally in terms of velocity or acceleration) at multiple depths. Seismic downhole array data provide a unique source of information on actual soil

behavior and local site amplification (Chang et al., 1996; Elgamal et al., 2001; Ysujihara et al., 1990; Wang et al., 2001). As the author and others (e.g. Elgamal et al. 1996; Stiedl et al. 1996) have pointed out over the years, vertical array data provides a direct way to quantify the accuracy of ground motion predictions, the models used to make such predictions, and the applicability of our estimates of in situ soil properties.

Downhole recordings of ground motion give us a glimpse of how waves are traveling near the surface of the earth. By comparing multiple downhole recordings and a related surface recording, one can observe how the waves change as they progress through the ground, encountering the materials in the soil profile. Part of the reason for placing the instruments below the surface is to reduce the effect of surface noise caused by cars, wind, and people. Another benefit of placing the instruments underground is to record the ground motion at additional points along the path of propagation. These arrays are changing the way we understand seismic ground motion by allowing the 3-D evaluation of seismic wave propagation (e.g. Baise and Glaser 2000; Stidham et al. 1999; Elgamal et al. 1996; Abrahamson et al. 1991).

We have developed several methods to interpret and understand data from vertical arrays (Glaser 1995; Ching and Glaser 2003a, 2003b, 2001). They range from linear to nonlinear to rapidly changing nonlinear models. We have found that all three approaches model the same data excellently. This paper will very briefly look at the linear and nonlinear (Bayesian inference) approaches, and then discuss the seeming contradiction of both being “correct.” In order to study the issues further we need more vertical arrays with finer granularity, which leads us to propose a new, inexpensive, and easy to install vertical array comprised of local embedded systems based on MEMS sensors and local microcontrollers

## LOTUNG, TAIWAN, VERTICAL SEISMIC ARRAY

In the early 1980's, the Electric Power Research Institute (EPRI) and the Taiwan Power Co. constructed two scale models (1/4 and 1/12 scale) of a nuclear containment structure near Lotung, Taiwan, a very seismically active area in northeast Taiwan (Tang, 1985). The site and structures were elaborately instrumented so that soil and structural response, and soil-structure interaction could be carefully studied during earthquakes (Tang et al., 1989). The instrumented site is commonly referred to as the LSST array.

The soil instrumentation at the LSST site includes a three-arm surface array with arms radiating approximately 47 m from the 1/4 scale containment structure (Tang, 1987). In addition, there are two down hole arrays of accelerometers extending to a depth of 47 m. The surface sensors are triaxial force-balance units (Kinometrics FBA-13) oriented in the N-S, E-W, and vertical directions. The down hole arrays (DHA and DHB) are modified Kinometrics FBA-13H units oriented in the N-S, E-W, and vertical directions. DHA is located 3 m from the 1/4 scale structure and DHB is located 47 m from the structure, allowing identification of the effects of the structure on soil response. The down hole instruments are located at depths of 6 m, 11 m, 17 m, and 47 m.

The geology of the Lotung site is summarized by Wen and Yeh (1984) and Tang (1989). The area consists of a recent alluvium layer 40 to 50 m thick overlying a Pleistocene formation that varies from 150 to 500 m in thickness. Underlying the Pleistocene material is a Miocene basement rock. A simplified soil profile consists of 30-35 m of silty sand and sandy silt with some gravel, above clayey silt and silty clay. The site has been extensively investigated (Anderson, 1993; Anderson and Tang, 1989) with five independent testing programs.

Of the 17 earthquakes recorded at the LSST site (Glaser and Baise, 2000; Anderson, 1993; EPRI, 1989), Events 4, 7, 12, and 16 will be considered “large” events, with peak accelerations over 0.17 g. Events 12 and 16 were major events and have been discussed in detail in the literature (e.g. Glaser and Baise, 2000; Chang et al., 1996; Zeghal et al., 1995; Anderson, 1993). Of these four large events, temblors 7 and 16 were deep focus events, and Event 12 was an event occurring nearby at shallow depth. The event of interest here, Event 16, at an epicentral distance of 78 km and a focal depth of 7 km, resulted in a peak ground acceleration of 0.17 g at the LSST.

### **JINGLIAO, TAIWAN, VERTICAL SEISMIC ARRAY**

Compared with the LSST array, the Jingliao down hole instrumentation is a small scale array. The site is located at Jingliao, Houbi, Tainan, Taiwan (see Fig. 1), and was selected expressly for monitoring local liquefaction down hole array instrumentation. The soil at the site (a rice field) liquefied in many places during the  $M_R$  6.4 October 22, 1999, Chiayi earthquake (one month after the Chi-Chi earthquake). A picture of an example sand boil is shown in Fig. 2. The array is located beside the Bachang River, and the ground water table is less than two meters below surface level. The site is surrounded by the Meishan fault, Chukou fault and Hsinhua fault. The soil deposits are part of the Chia-Nan Plain, the coastal plain of western Taiwan, and consist of alluvial deposits of clay, silt, sand, and gravel. Detailed Cone Penetration testing indicates that the alluvial soils are loose with some intervals very susceptible to liquefaction.

The array, installed in August, 2003, consists of four accelerometer sets, four piezometers, and a Sondex displacement measuring system. All data is digitized at a rate of 512 samples/second. Three sets of three-component accelerometers are installed at the site, each in a separate bore – one set at the surface, one at 8.2 meters deep, one at 10.5 meters deep, and

another at a thirty one meter depth. The triaxial accelerometers used are manufactured by Tokyo Sokushin Co., with model VSE-355T installed at the surface and model VSE-355 in the subsurface. The frequency response of these accelerometers is from 0.018 to 100 Hz. with a linearity of 0.03% full scale, a range of  $\pm 2$  g, and a sensitivity of 5 V/g.

Two holes were bored for installation of the piezometers which will monitor generation of excess pore water pressure during earthquake shaking. Piezometers were installed at four and eleven meters in one hole, and at fifteen and twenty four meters in the other. The pore water pressure transducers are Tokyo Sokushin Co. model PWG-35Gi. The range of measurement is 0 ~ 3.5 kgf/cm<sup>2</sup> with 0.5 % full scale linearity and a response time constant of 2 msec.

To measure the ground settlement induced by soil liquefaction, a Slope Indicator Co. Sondex settlement monitoring system, model 50819, was installed. The system accuracy is  $\pm 0.1$  inches relative to the cable marks. A total of thirteen sensing points (depths) were placed in the borehole. The depths are 2.234, 3.218, 4.214, 6.102, 7.805, 8.053, 9.974, 10.976, 11.988, 13.854, 14.854, 15.865, 17.733 meters respectively. The relative deformation among the sensing points is monitored.

## **SYSTEM IDENTIFICATION OF VERTICAL ARRAY DATA**

### **System Parameter Modeling**

It has been widely accepted that during small earthquakes the process between two points in a downhole-uphole array is roughly equivalent to a linear filter (e.g. Schnabel et al 1976; Ching and Glaser 2001). This concept manifests itself by the Fourier-type analyses (e.g. Fourier spectral ratio, cross spectrum, etc.) used in the context of nonparametric modeling (e.g. Schnabel et al. 1972), and by an infinite impulse response (IIR) filter (e.g. Glaser 1995) in the context of parametric modeling. The two approaches seem very different but their goals are

identical: to identify dynamic soil properties by estimating the linear filter that maps one signal to the other signal.

The parametric technique used here falls into the category of site response estimation but differs significantly from the standard spectral ratio methods. The empirical Green's functions we derive from an inversion of input-output ground motion data sets have predictive value in that they can directly be used to predict future surface ground motions given an input ground motion. Given input and output vibration data from a vertical seismic array, the system parameter estimation of an empirical Green's function is attempting to capture the same quantity as a spectral ratio of the two records - a mapping of shaking time histories between two points in the soil profile. The system parameter estimation method used here estimates the mapping directly as weights of an IIR filter. Spectral-based methods directly estimate the weights and phase-shifts for a given trigonometric infinite series - the transfer function estimate is a secondary step. When using spectral ratios, the recommended procedure is to average spectra from multiple events at the same site, and window and smooth the data (in both time and frequency domains) to reduce the noise and uncertainties, and identify the correct spectra.

In our approach, we can make use of single earthquake events, and essentially take an extended Wiener approach (the minimum-phase constraint is given up, at the cost of possible instability of the recursive function). The relative advantages (and disadvantages) of the Wiener-based methods compared to spectral ratios have been extensively discussed in the signal processing and control theory literature (e.g. Wiener 1964; Berg 1975; Jurkevics and Ulrych 1978; Cakmak and Sherif 1984). The result is a linearly-scaled time series, and is compared to actual results. We also chose the system parameter method for the ease of formulating a prediction model.

System parameter modeling involves inversion of input and output data for a statistical, parametric model of a predetermined form. A simple model for characterizing a system is a polynomial mapping between system input and output. One such model, referred to as an autoregressive-moving average model with exogenous noise, characterizes the system as a weighted polynomial of past outputs (AR) and past and present inputs (MA) (e.g. Kanasewich 1981) with noise added as a direct term without weights. There is some confusion about the naming of this type of model. In deference to Prof. Ljung (1987), we refer to the following as an AR model.

$$y_i = a_1 y_{i-1} + a_2 y_{i-2} + \dots + a_{na} y_{i-na} + b_1 x_{i-1} + \dots + b_{nb} x_{i-nb} + e_i = \sum_{j=1}^{na} a_j y_{i-j} + \sum_{j=1}^{nb} b_j x_{i-j} + e_i \quad (1)$$

where  $y$  is the actual output data sequence,  $x$  is the input sequence,  $a$ 's and  $b$ 's are the AR and MA parameters, respectively,  $e$  is the noise term, and the subscript is the time step counter. The output is seen as a combination of the input history acted upon by the “ $b$ ” coefficients and the past outputs acted upon by the “ $a$ ” coefficients. The input series, involving the “ $b$ ” coefficients, is a non-causal moving average (MA) feed-through process (convolutional). The series involving weighted past output values (“ $a$ ” coefficients) is a causal autoregressive (AR) process. The input and output time histories both contain all motions at their respective locations including reflections (downgoing and upgoing waveforms). The reflections (from stratigraphy) are a site property and are inherently accounted for by the inverse model. In fact, it has been shown by several authors (Goupillaud 1961; Claerbout 1968; Robinson and Treital, 1978) that seismic transmission through a layered system (e.g. stratigraphic column) is an autoregressive process.

Extensive analysis of vertical array data from more than a half-dozen sites (Baise and Glaser, 2000) has shown that the linear IIR approach works extremely well as a predictive tool. An

example is from the results of the Port Island array for the 1995 Hyogo-ken Nanbu Earthquake (Baise et al., 2001). Using the methodology discussed, EGFs were determined for intervals A, B, and C for the 28 June, 1994 foreshock (MJMA = 4.6; PGA = 0.007 g). The filter for the 32 m to 16 m interval (interval B) was then applied to the main-shock data entering at 32 m (MJMA = 7.2; PGA = 0.54 g) in order to estimate the 16 m deep response. As shown in Fig. 3, the predicted result matched well, with a normalized error of 0.09.

### Nonlinear Analysis Using Bayesian Inference

The Fourier-type spectral estimation for a single waveform is notorious for the associated uncertainties (Marple and Lawrence 1987). In order to reduce the uncertainties, regularization, including smoothing and windowing in time/frequency domain, is inevitable. This regularization reduces uncertainties by introducing bias into the estimates. For a short noisy signal, the IIR filter modeling is superior to the Fourier-type analysis for the purpose of spectral estimation (Marple and Lawrence 1987) in the sense that (1) many fewer parameters are required and (2) the uncertainties associated with the estimates are smaller. Therefore we adapted the IIR filter approach into a Bayesian inference scheme to model relatively slow-changing nonlinearities in the soil system (Ching and Glaser, 2003).

One way of modeling nonlinear soil behaviors is to allow the filter coefficients ( $a$ 's and  $b$ 's in Eqn. 1) to change with time, i.e.

$$y_t = a_1(t)y_{t-1} + a_2(t)y_{t-2} + \dots + b_1(t)x_{t-1} + \dots = \sum_{j=1}^{na} a_j(t)y_{t-j} + \sum_{j=1}^{nb} b_j(t)x_{t-j}, \quad (2)$$

or simply:

$$y_t = C_t^T \Phi_t, \quad (3)$$

where  $C_t^T$  is the data vector  $[y_{t-1} \ y_{t-2} \ \dots \ y_{t-na} \ x_{t-1} \ x_{t-2} \ \dots \ x_{t-nb}]$ , and  $\Phi_t^T$  is the parameter vector  $[a_1(t) \ a_2(t) \ \dots \ a_{na}(t) \ b_1(t) \ b_2(t) \ \dots \ b_{nb}(t)]$ . We can then model the entire process taking place between each accelerometer pair on the string as a set of stochastic state-space equations,

$$\Phi_t = \Phi_{t-1} + w_t \quad y_t = C_t^T \Phi_t + v_t, \quad (4)$$

where  $\{w\}$  and  $\{v\}$  are noise terms with variance  $\{Q\}$  and  $\{R\}$  respectively. Here  $\{w\}$  denotes  $\{w_t; t=1,2,\dots,T\}$ , and similar for  $\{v\}$ ,  $\{Q\}$ , and  $\{R\}$ . The first equation governs the fluctuation of system parameters through time. The degrees of freedom of fluctuation at time  $t$  are specified by the size of  $Q_t$ . The second equation is the IIR filter equation with additive noise  $v_t$ . The uncertainties that cannot be captured by the IIR filter equation at time  $t$  are lumped into  $v_t$ . The uncertainties can include measurement noises, the modeling errors of Eqn. 2, and numerical errors.

We assume  $\{w\}$  and  $\{v\}$  to be independent (within and between) jointly Gaussian for two reasons: (1) independent normal distributions maximize the differential entropy (Cover and Thomas 1991), hence minimize the constraints imposed on the data by our model and (2) if we also assume  $\Phi_0$  normally distributed and  $\{C\}$  deterministic,  $\{\Phi\}$  will be jointly Gaussian because  $\{w\}$  and  $\{v\}$  are jointly Gaussian. This makes the problem computationally feasible.

## **EXAMPLES OF SYSTEM IDENTIFICATION FROM VERTICAL ARRAY DATA**

### **Example results from the Lotung Vertical Array, Taiwan**

An example of the predictive ability of the system parameter (linear IIR) model is shown in Fig. 4. The actual velocity time history from the six meter to surface interval for DHB in the north-south direction, and is compared to the prediction made through a 4,4 model derived from Event 9. The goodness of fit shown in Fig. 4 is representative for the model fits for Events 3, 4, 7, 8, 9, 10, 12, 16 for the four successive depth intervals. From the filter parameters of the 4-4 ARMA model used, the calculated stiffness was 2.9 MN/m and the viscous damping ratio was 18% of critical.

Event16, DHB N-S, was also analyzed by the nonlinear Bayesian inference technique. With this model the material properties are allowed to change through time, and therefore with strain so that we can estimate the modulus degradation curve and damping curve from a strong enough single event. We found that all strong events show substantial soil degradation. As an example, Fig. 5 shows the interval's estimated shear velocity time history of Event 16, six m to surface interval. From the estimated interval shear velocity, the shear stiffness can be calculated and the value at each moment in time is associated with the soil strain at that point, yielding a shear modulus degradation curve for the full range of strains experience in that temblor. This is shown in the right-hand graph in Fig. 5. It is clear that the inferred soil stiffness decreases with the intensity of ground motion, as is expected. The Bayesian method allows the soil damping to be calculated through time as the model parameters change. The model uses the viscous damping ratio as the measure of damping, and the time evolution for the Event16 is presented in Fig. 6. The damping ratio more than doubles during the period of strong shaking, returning to a near-undisturbed value with the coda. In summary, the soil degradation curves from all strong events recorded at Lotung are shown in Fig 7. Comparison with work by Chang et al. (1996) shows that the identified values for the active portion of shaking (before the Coda) tracks Chang's estimates for the degradation curve, and shows how well the Bayesian method works to estimate shear degradation due to dynamic strain. It is interesting to notice that the inferred natural frequencies do not return to their initial values near the end of the event.

The question emerges as to why both a linear and nonlinear mapping identifies soil behavior so well. In actuality the problem is not well constrained – we have only acceleration data at a few points in the profile, and many models can fit the data through them. The ones chosen here are satisfying because the models are parsimonious and the parameters have a physical link to vertical wave propagation in a layered medium. One way to increase constraints is by

more densely instrumenting sites, with several accelerometer stations in each stratum. To do this in an affordable fashion requires a new type of downhole array – TerraScope.

### **Example results from the Jingliao Vertical Array, Taiwan**

The Jingliao data analyzed in this paper are from two earthquake events. The first event was scaled at a Richter magnitude of 4.6 and occurred on 12 April, 2005. The epicenter was located about 4.5 km to the east of the Doneshan Station, Tainan, and the hypocenter located at a depth of 5.2 km. The second event was scaled at a Richter Magnitude of 5.1 and occurred on June 4, 2006. The epicenter was located about 16.8 km northeast of the Taidone Station, while the hypocenter was located at a depth of 21.8 km.

For the Jingliao data an ARMAX (Auto-Regressive Moving Average eXogenous input, e.g. Ljung, 1987) model was implemented to model the soil system. For this model, the system filtering of the white noise itself is expressly considered and poles and zeros estimated. It can be written as

$$y_i = a_1 y_{i-1} + a_2 y_{i-2} + \dots + a_{na} y_{i-na} + b_1 x_{i-1} + \dots + b_{nb} x_{i-nb} + e_i + c_1 e_{i-1} + c_2 e_{i-2} + \dots + c_{nc} e_{i-nc} = \sum_{j=1}^{na} a_j y_{i-j} + \sum_{j=1}^{nb} b_j x_{i-j} + e_i + \sum_{j=1}^{nc} c_j e_{i-j} \quad (5)$$

Where  $e$  is white noise, and  $na$ ,  $nb$  and  $nc$  are the AR, MA, and white noise orders respectively. The input-output data for different soil intervals were analyzed by order two ( $na = nb = nc = 2$ ), order four, and order six models to obtain the identification.

The modal frequencies and damping ratios determined from the model poles (Ghanem, et al., 1991; Glaser, 1996) are shown in Table 1 and Table 2 respectively. The resonant frequency decreases with interval depth while the damping ration remains about the same. The behavior in the east-west direction and north-south direction exhibits similar trends, with the difference in resonant frequency between the E-W and the N-S direction about 0.3 Hz for the top interval,

and close to the same for the deepest interval. The resonant frequencies of the Event-2006-06-04 are near identical to those of the Event-2005-04-12. From the Table 2, it can be known that the damping ratio of this site is about 8%~15%. The interlayer stiffness can be estimated from the identified parameters. Estimates of shear wave velocity and shear wave modulus for the Jingliao site are given in Table 3. The resulting model parameters were “checked” by comparison to resonant column testing. The model-estimated parameters should not be the same as from the resonant column tests because the boundary conditions are so different. The prime advantage of using vertical seismic array data is that the actual in situ responses are analyzed as opposed to the artificial strain and wave propagation boundary conditions enforced by testing disturbed laboratory specimens.

### **THE TERRASCOPE SYSTEM**

At this point the case has been made that important information about soil dynamics and site response can be made from the unique data provided by vertical seismic arrays. Vertical arrays have traditionally been very expensive to install and maintain (Steidl and Nigbor 2001; Steidl 2005), being much like traditional structural seismic instrumentation. They suffer from a limited functionality, high cost of instrumentation, and size. Some vertical arrays utilize a separate borehole for each instrument, others install multiple instruments into one hole, but both require more complex ancillary systems, which increase the total cost tremendously. Also, for these systems, the data collection and management is inconvenient. The data are collected locally in the field, so it is inconvenient to expand the network, and the data can not always be made available to the public as the events occur

We constructed a field-deployable vertical seismic array that can be installed in a variety of manners. Initially the arrays will be installed into uncased (or cased) boreholes. We can envision when the arrays will be inserted into the ground by ubiquitous cone penetrometer

equipment. The TerraScope system, as outlined in Fig. 8, is comprised of several interacting parts. The array itself is composed of a number of independent sensor Pods dispersed in a borehole, and linked by thin wire to a base station. The base station, while systemically independent from the local gateway, is housed within the same enclosure as the gateway.

### **The Pod**

The “Pod” is the active independent down-hole measuring device that is the heart of TerraScope, a picture of which is shown in Fig. 9. Each Pod is an independent, microprocessor-controlled agent with four or more Mb of non-volatile memory. The system is designed to implement the following:

- Integration of advanced technology accelerometers ( $75 \text{ ng}_{\text{rms}}/\sqrt{\text{Hz}}$  noise floor, 24-bit  $\delta$ - $\Sigma$  force-balance); a second set of accelerometers extends dynamic range to 2 g;
- Tilt (pitch and roll) with 0.003 degree repeatability;
- Azimuth  $\sim$  1 degree repeatability;
- Real-time clock to within 0.5 ms;
- Parametric measurands can include temperature, pH, pore water pressure, etc.;
- Recording all of dynamic variables at a digitization rate of 100 Hz for at least one minute before trigger and two minutes after;
- Fully dynamic networking, real-time reprogramming, and peer-to-peer sensor fusion.

### **Application Specific Embedded System**

The TerraScope system is used to measure seismic signals traveling through soil and rock. Given that these are very dispersive materials, the frequencies of interest are very low, up to about fifty Hz at the most. To cover any eventualities such as structural monitoring, and to

facilitate improvement is signal to noise ratio through oversampling, the design criteria is to allow digitization rates of up to 250 samples per second, or a  $\Delta t$  of four ms. For a digital system running at eight MHz, this data rate can be considered relatively slow and many tasks ordered and completed between sampling. Figure 9 depicts the system architecture. The nominal one minute pre-trigger segment insures that motion occurring before strong shaking is captured. A nominal two-minute post-trigger recorded segment insures that all motions and aftershocks are recorded. The system is designed so that a second three-minute event set be recorded to a second bank of SRAM while the first segment downloads independent of system operation

Once a vertical array is buried in its borehole, it is unreasonable to retrieve it for repair or updating. The prime design consideration is the insurance of retrieving accurate time-stamped acceleration data. To this end we have incorporated a second digital bus to the MCU, which serves two purposes. Its main purpose is to allow dynamic reprogramming of each Pod. This allows for updates of firmware, as well as changes and extension of mission. This bus also serves as a “back door” to the Pod system to allow external downloading of memory in an emergency.

Each base station is the command center for an array; multiple hardware Pods are suspended on a bus cable at different levels, synchronized with the local gateway global timer, sample data, and communicate with the base station. A cartoon of the architecture is presented in Fig. 9. A slim cable of four twisted conductor pairs provides both physical connection and communications channels between the Pods and the base station. For security, one pair of conductors is reserved for twelve volt power, one for bidirectional communications, a third for sync timing, and a fourth for dynamic reprogramming. The main responsibility of the base station is to (1) send the real time clock to the Pods, (2) connect the Pods to the outside world

by sending and relaying commands from the embedded system to the Linux machine for data exchange through the RS232 serial port. The Linux machine is a single board computer running an embedded version of the Red Hat Linux operating system. It connects the users/operators and the system via a web server to allow remote and effortless interaction over the Internet. This is accomplished by running two concurrent applications, one interacting with the base station embedded system and the other a GUI web interface to interact with the user.

A photograph of the finished product is shown in Fig. 10, with the major sensing systems highlighted. The major cost of the device is the ultra-low-noise accelerometer module, which costs \$3000. The total cost of the pod could be reduced by over \$2500 by utilizing more inexpensive devices that have a higher noise floor, say 50  $\mu\text{g}$ . A prototype device has been recently installed under the watchtower at the top of Masada mountain in Israel. Data can be examined with an interactive tool online at [www.ce.berkeley.edu/~glaser/masada.html](http://www.ce.berkeley.edu/~glaser/masada.html). The device is currently undergoing field evaluation and will be replaced by a newer prototype in December of 2006.

## CONCLUSIONS

We have presented two stationary ARMA-based schemes and one nonlinear Bayesian inference method to model the site response using data from vertical seismic arrays. The stationary methods use a linear infinite impulse response filter, one modeling the noise as a direct term and the other mapped through filter coefficients. Both methods do an excellent job in blind prediction of site response to a known input signal. All three methods allow quantitative estimation of interval parameters such as stiffness and viscous damping ratio. The fact that both a linear and a nonlinear model make such excellent blind predictions of site response begs the question as to whether the soil system responds “linearly” or “nonlinearly.” It is conjectured that many different models can match a set of data, especially if there is a

paucity of physical constraints, such as we have. A possible solution to this lack of sufficient information is to install much denser vertical arrays in a three-dimensional grid, with multiple accelerometers in each stratum.

Two vertical seismic arrays were introduced: the LSST array in Lotung, Taiwan, and the Jingliao array in Jingliao, Tainan, Taiwan. The Lotung array consists of two strings, each with accelerometer stations at 6, 11, 17, and 47 depth, while the Jingliao array has stations at 8.2, 10.5, and 31 meters deep. The Jingliao array also has piezometers at four, eleven, fifteen, and twenty four levels. There is also one Sondex system installed to measure vertical displacements. The input-output soil models used to make the presented accurate estimates of dynamic soil properties requires the use of vertical seismic arrays. A current limitation to installing mainly is the enormous cost of traditional vertical arrays. We present TerraScope as a solution to this problem. TerraScope is an inexpensive but extremely accurate vertical array system based on MEMS sensors and local microprocessing power. It is expected that each Pod will measure from  $75 \text{ ng}_{\text{rms}}/\sqrt{\text{Hz}}$  to 1.7 g full scale with direct digital accelerometers, and cost about \$6000. In addition each pod will measure tilt, azimuth, and can measure other parametric data such as pore water pressure.

#### **ACKNOWLEDGMENTS**

I would like to acknowledge NSF grant CMS-0301797 for making this work possible. The Lotung modeling is from the work done by Profs. Laurie G. Baise (Tufts University) and Jianye Ching (National Taiwan University of Science and Technology). They were the stars, I was only the coach. Special thanks go to Dr. Win-Gee Huang from Institute of Earth Science, Academia, Sinica for providing much of the data from the Lotung array.

## REFERENCES

- Anderson, D.G. (1993), *Geotechnical synthesis for the Lotung large-scale seismic experiment*, Report TR-102362, Palo Alto: Electric Power Research Institute.
- Anderson, D.G. and Tang, Y.K. (1989), “Summary of soil characterization program for the Lotung large-scale seismic experiment,” *Proceedings: EPRI/NRC/TPC workshop on seismic soil-structure interaction analysis techniques using data from Lotung, Taiwan*, Report NP-6154
- Baise, L.G. and S. D. Glaser, S.D. (2000), “Consistency of site response estimates made using system identification,” *Bulletin, Seismological Society of America* **90**(4), 993-1009.
- Baise, L.G., S.D. Glaser, S.D. and T. Sugano, (2001), “Consistency of dynamic site response at Port Island,” *Earthquake Engineering and Structural Dynamics* **30**(6), 803-818.
- Berg, J. P. (1975), *Maximum entropy spectral analysis*. Ph.D. thesis, Stanford University.
- Cakmak, A. S. and Sherif, R. I. (1984), “Parametric time series models for earthquake strong motions and their relationship to site parameters,” *Proc. 8th World Conference on Earthquake Engineering II*, 581-588.
- Chang, C.-Y., Mok, C.M. and Tang, H.T. (1996), “Inference of dynamic shear modulus from Lotung downhole data,” *ASCE Journal of Geotechnical Engineering* **122**(8), 657-665.
- Ching, J.-Y. and Glaser, S.D. (2003a), “Identification of soil degradation during earthquake excitations by Bayesian inference,” *Earthquake Engineering and Structural Dynamics* **32**, 845–869.
- Ching, J.-Y. and Glaser, S.D. (2003b), “Tracking rapidly changing dynamical systems using a semi-parametric statistical method based on wavelets,” *Earthquake Engineering and Structural Dynamics*, **32**, 2377–2406.

- Ching, J.-Y. and Glaser, S.D. (2001), "Time domain solution of 1-D shear wave propagation in layered media," *ASCE Journal Geotechnical Engineering* **127**(1), 36-47.
- Claerbout, J.F. (1968), "Synthesis of a layered medium from its acoustic transmission response," *Geophysics* **33**, 264-269.
- Cover, T.M. and Thomas, J.A. (1991), *Elements of information theory*. John Wiley and Sons, New York.
- Elgamal, A.-W., Zeghal, M., Parra, E., Gunturi, R., Tang, H.T. and Stepp, J.T. (1996), "Identification and modeling of earthquake ground response – I. Site amplification," *Soil Dynamics and Earthquake Engineering* **15**, 499-522.
- EPRI (1989), *Proceedings: EPRI/NRC/TPC workshop on seismic soil-structure interaction analysis techniques using data from Lotung, Taiwan*, Vol. 1 & 2, Report NP-6154.
- Ghanem, R.G., Gavin, H. and Shinozuka, M. (1991), "Experimental Verification of a number of structural system identification algorithms," *Technical Report NCEER-91-0024*, p. 302.
- Glaser, S.D. and L.G. Baise (2000), "System identification estimation of soil properties at the Lotung site," *Soil Dynamics and Earthquake Engineering* **19**(6), 521-531.
- Glaser, S.D. (1995), "System identification and its application to estimating soil properties," *ASCE Journal of Geotechnical Engineering* **121**(7) 553-560.
- Glaser, S.D. (1996), "Estimation of System Damping at The Lotung Site by Application of System Identification," *NIST GCR 96-700*, National Institute of Standards and Technology, Gaithersburg, MD.
- Goupillaud, P.L. (1961), "An approach to inverse filtering of near-surface layer effects from seismic records," *Geophysics* **26**(6), 754-760.

- Jurkevics, A. and Ulrych, T. J. (1978), "Representing and simulating strong ground motion," *Bulletin of the Seismological Society of America* **68**(3), 781-801.
- Kanasewich, E. (1981), *Time Sequence Analysis in Geophysics*. Edmonton, Alberta: U. Alberta Press.
- Ljung, L.J. (1987), *System identification: theory for the user*. Englewood Cliffs, NJ: Prentice-Hall
- Marple, L. Jr. and Lawrence, S. (1987), "*Digital spectral analysis with applications*," Englewood Cliffs: Prentice-Hall.
- Robinson E. and Treital, S. (1978), "The fine structure of the normal incidence synthetic seismogram," *Geophysics Journal of the Royal Astronomical society* **53**, 289-309.
- Schnabel, P. B., Lysmer, J. and Seed, H.B. (1972), "SHAKE, A computer program for earthquake response analysis of horizontally layered sites," Berkeley, CA: *Earthquake Engineering Research Center*. (No. 72-12)
- Stidham, C., Antolik, M., Dreger, D., Larsen, S. and Romanowicz, B. (1999), "Three-dimensional structure influences on the strong-motion wavefield of the Loma Prieta earthquake," *Bulletin of the Seismological Society of America* **89**(5), 1184-1202.
- Steidl, J., Tumarkin, A.G. and Archuleta, R. (1996), "What is a reference site," *Bulletin of the Seismological Society of America* **86**, 1733-1748.
- Steidl, J. and Nigbor, R. (2000), *SCEC/ROSRINE Workshop on borehole array data utilization*, Palm Springs, CA, 16 Dec.
- Steidl, J. (2005), *Personal communication*.
- Tang, H.T. (1987), "Large-scale soil-structure interaction," *Report NP-5513-SR*. Palo Alto: Electric Power Research Institute.

Tang, H.T., Tang, Y.K., Stepp, J.C., Wall, I.B., Lin, E., Cheng, S.C., Lee, S.K. and Hsiau, H.M. (1989), “EPRI/TPC large-scale seismic experiment at Lotung, Taiwan,”

*Proceedings: EPRI/NRC/TPC workshop on seismic soil-structure interaction analysis techniques using data from Lotung, Taiwan, Report NP-6154, Palo Alto: EPRI.*

Wen, K.L. and Yeh, Y.T. (1984), “Seismic velocity structure beneath the SMART 1 array,” *Bulletin of the Institute of Earth Science, Academia Sinica*, 4.

Wiener, N. (1964), *Extrapolation, interpolation and smoothing of stationary time series*, M.I.T. press.

Zeghal, M., Elgamal, A.-W., Tang, H.T., and Stepp, J.C. (1995), “Lotung downhole array: evaluation of soil nonlinear properties,” *Journal of Geotechnical Engineering*, 121(4), 363-378.

Table 1 Fundamental resonant frequencies.

Event	Frequency (Hz)			
	2005/04/12		2006/06/04	
Direction	EW	NS	EW	NS
8.2m~0m	4.6	4.3	4.3	4.2
10.5m~0m	3.9	3.7	-	-
10.5m~8.2m	3.8	3.7	-	-
31m~0m	2.0	2.1	1.9	1.9
31m~8.2m	2.0	2.0	1.8	1.9
31m~10.5m	2.0	2.0	-	-

Table 2 Damping ratio.

Event	Damping ratio			
	2005/04/12		2006/06/04	
Direction	EW	NS	EW	NS
8.2m~0m	10.03	13.11	10.64	12.39
10.5m~0m	15.40	11.65	-	-
10.5m~8.2m	13.14	8.09	-	-
31m~0m	9.06	9.90	12.03	11.01
31m~8.2m	10.89	10.71	14.24	12.83
31m~10.5m	13.89	12.61	-	-

Table 3 Shear velocity and estimated shear modulus for the Jingliao site.

Orientation	Shear velocity (m/s)		Shear modulus (MPa)	
	EW	NS	EW	NS
From 8.2m to 0m	142	136	40.8	37.2
From 10.5m to 0m	164	155	53.9	48.6
From 10.5m to 8.2m	240	225	112	98
From 31m to 0m	242	248	118.5	124.7
From 31m to 8.2m	278	288	155.6	167.8
From 31m to 10.5m	282	295	160.3	176.3

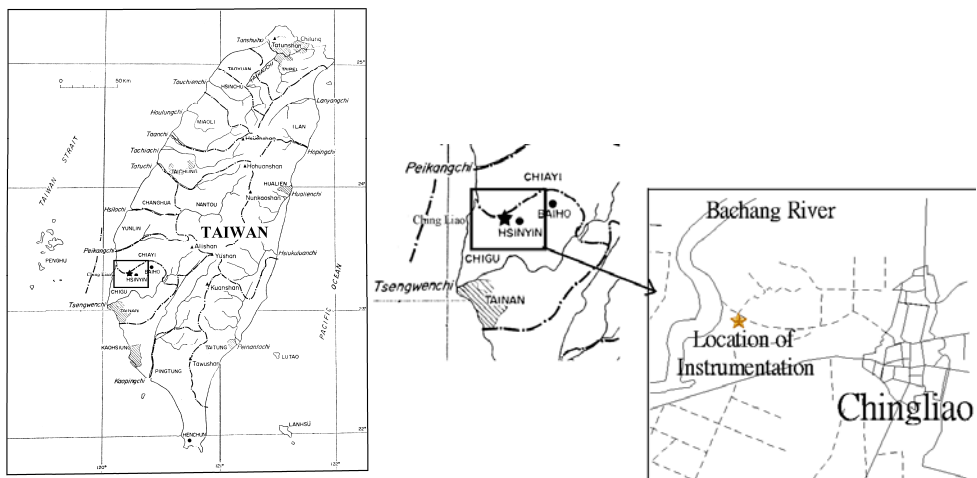


Figure 1 Location of Jingliao site

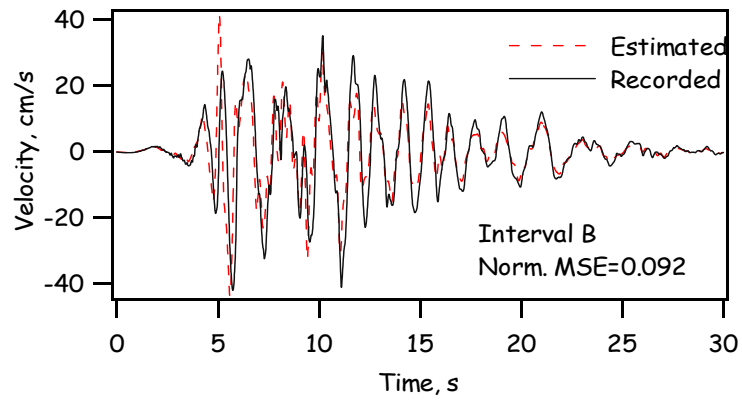


Figure 2 Sand boils in a rice field at Jingliao following the Chiayi earthquake

Figure 3 Comparison of the horizontal velocity time history blind prediction from the system parameter model and actual Hyogo-ken Nanbu event, 32 m to 16 m. The filter was generated from a small forshock.

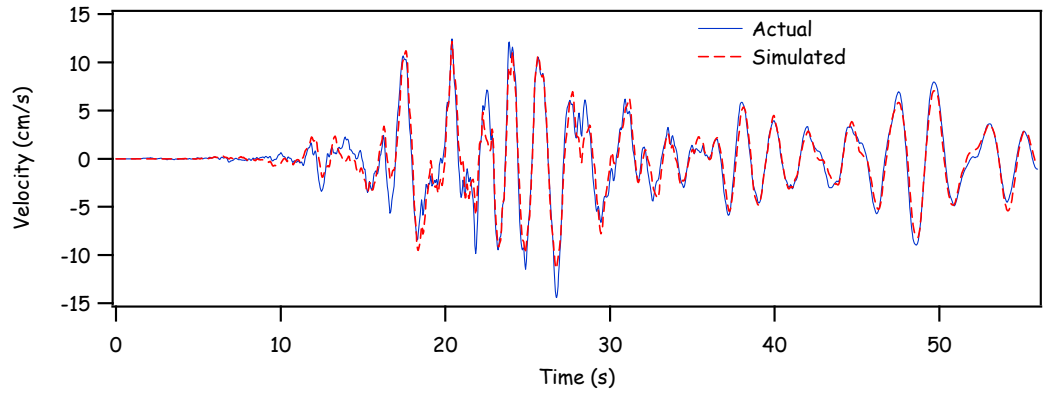


Figure 4 Blind prediction from a 4,4 IIR model compared to the actual interval output, Lotung Event 16 N-S, six m to surface interval.

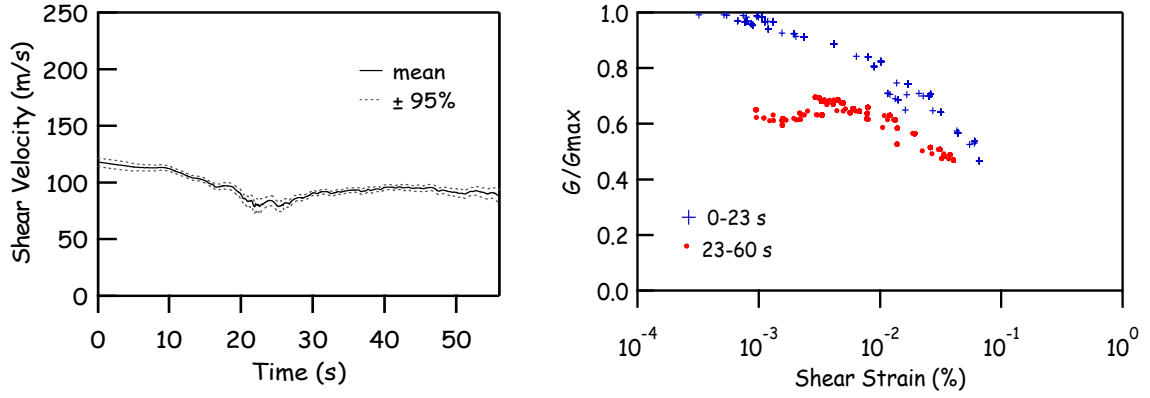


Figure 5 Evolution of inferred shear wave velocity and shear modulus degradation curve of LSST16, six m to surface.

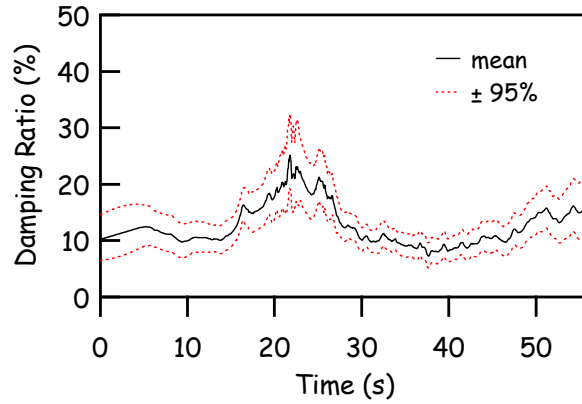


Figure 6 Evolution of the viscous damping ratio as a function of time for Lotung event 16, six m to surface, estimated by Bayesian inference.

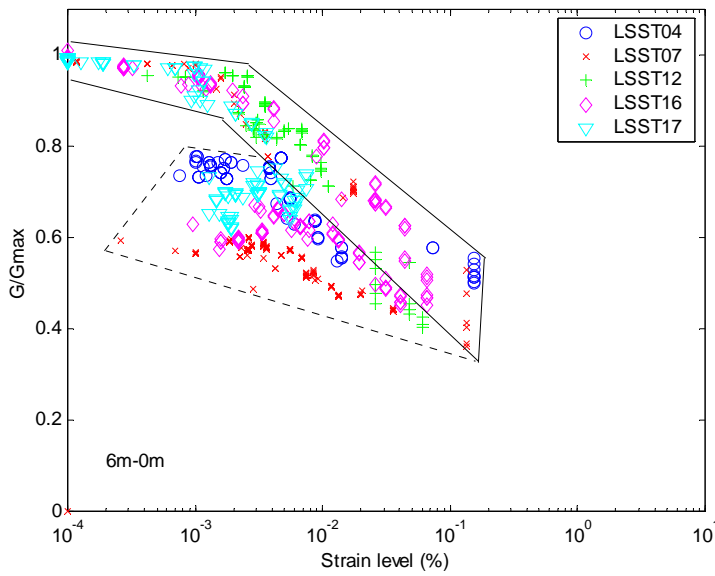


Figure 7 Compilation of degradation curves estimated by Bayesian inference for the 6m - surface interval of the Lotung array for five strong events. The solid line is the estimate for increasing strain, the dashed for the coda.

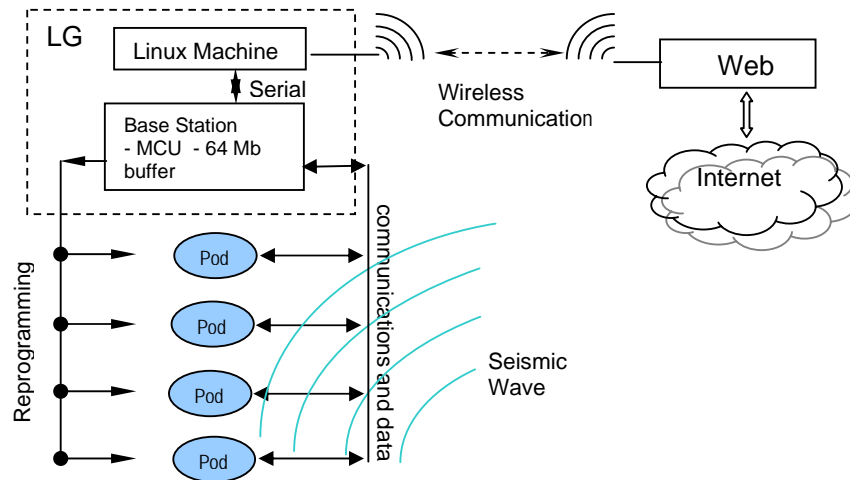


Figure 9 Cartoon of the TerraScope system architecture.

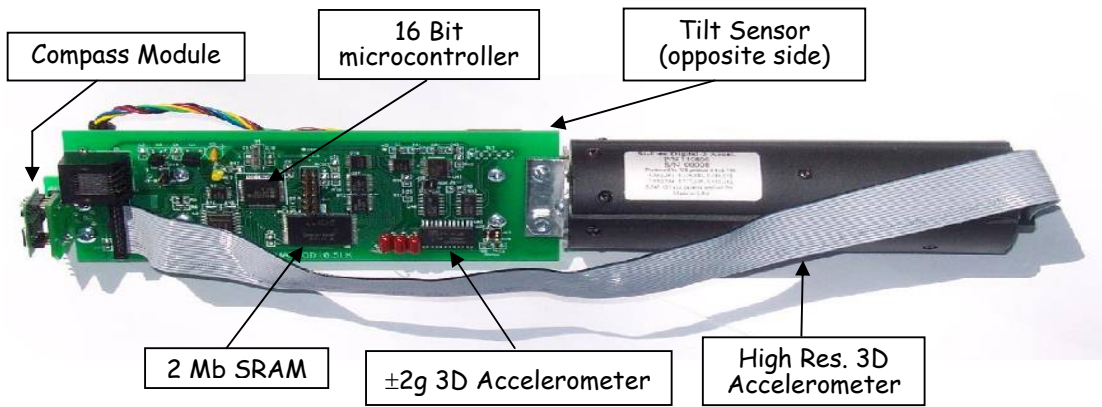


Figure 10 A photograph of the current TerraScope prototype that is installed at Masada Mountain, Israel.